

Supplementary material

Design of Three-dimensional Hierarchical TiO₂/SrTiO₃ Heterostructures towards Selective CO₂ Photoreduction

Shuaiyu Jiang,^{a†} Kun Zhao,^{a†} Mohammad Al-Mamun,^a Yu Lin Zhong,^a Porun Liu,^a Huajie Yin,^a Lixue Jiang,^a Sean Lowe,^a Jian Qi,^b Ranbo Yu,^c Dan Wang,^{a,b*} and Huijun Zhao^{a*}

^a*Centre for Clean Environment and Energy, Gold Coast Campus, Griffith University, QLD 4222, Australia.*

^b*State Key Laboratory of Biochemical Engineering, CAS Center for Excellence in Nanoscience, Institute of Process Engineering, Chinese Academy of Sciences, Zhongguancun, Beijing, China.*

^c*Department of Physical Chemistry, School of Metallurgical and Ecological Engineering, University of Science and Technology Beijing, Beijing 100083, China.*

*Correspondence and requests for materials should be addressed to D. W. (email: danwang@ipe.ac.cn), H. Z. (email: h.zhao@griffith.edu.au).

†These authors equally contributed to this work.



Fig. S1 Digital photograph of CO₂ photocatalytic reduction equipment.

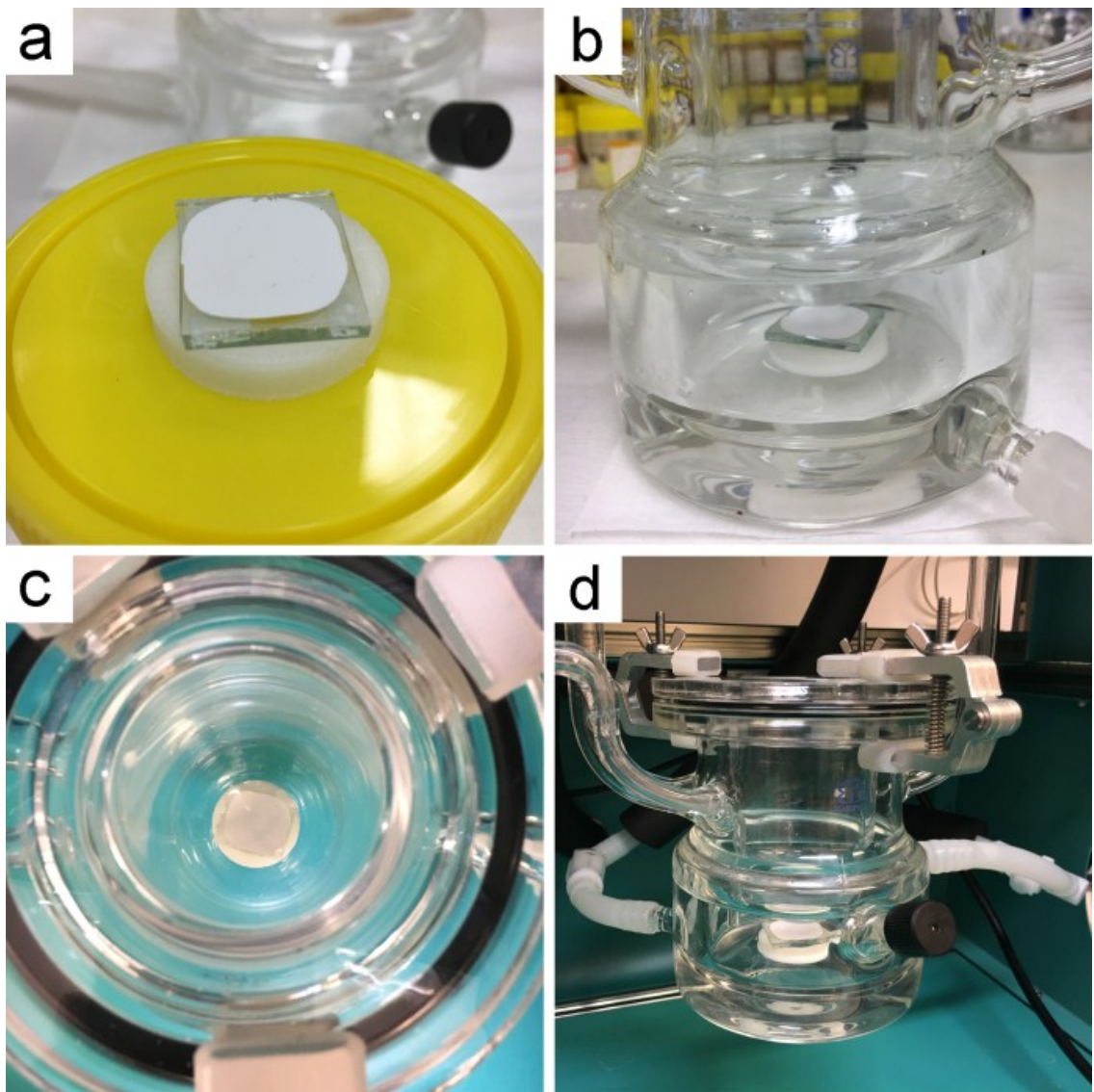


Fig. S2 The experimental setup for the gas-solid interface CO_2 reduction reactor with water.

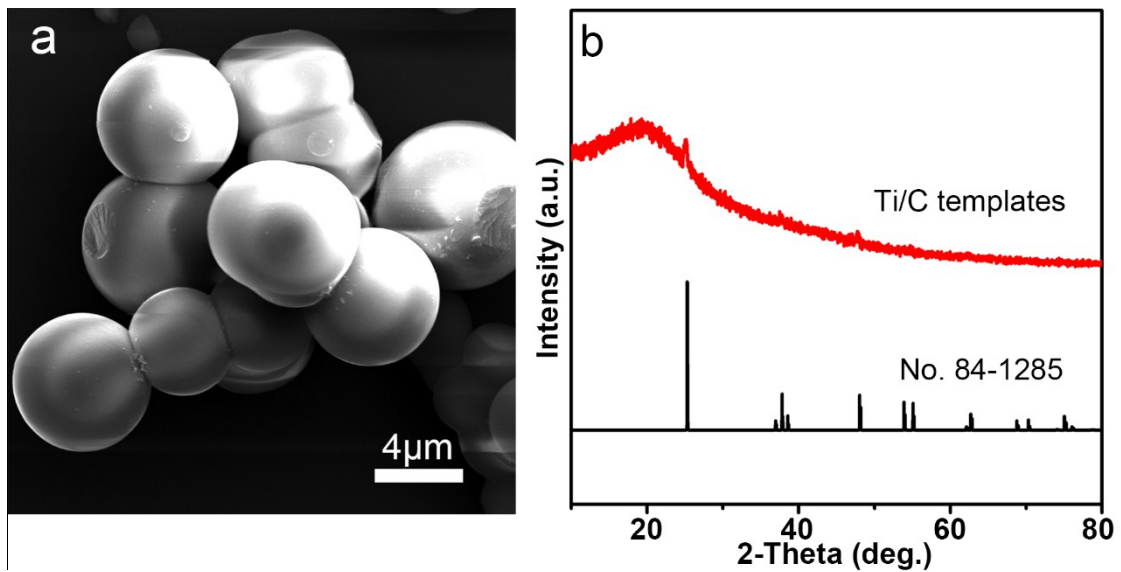


Fig. S3 (a) SEM image and (b) XRD pattern of as-synthesized composite titanium-carbon spherical templates.

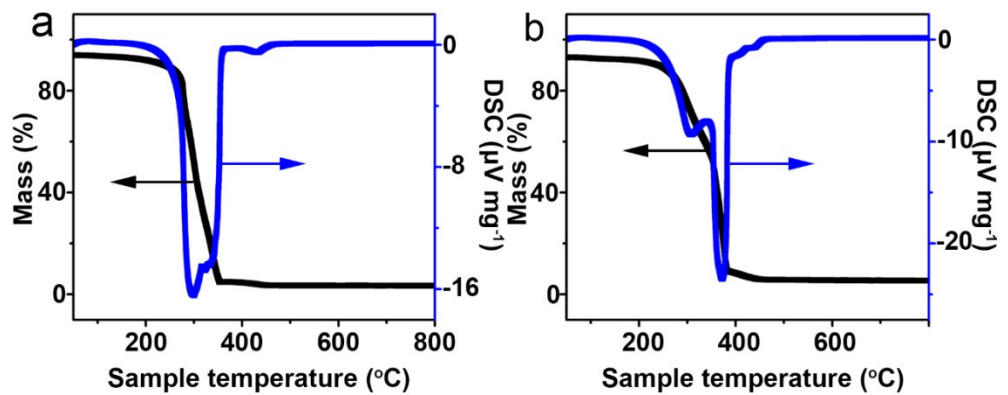


Fig. S4 TGA-DSC curves of (a) virgin Ti/C template and (b) Sr^{2+} adsorbed Ti/C template.

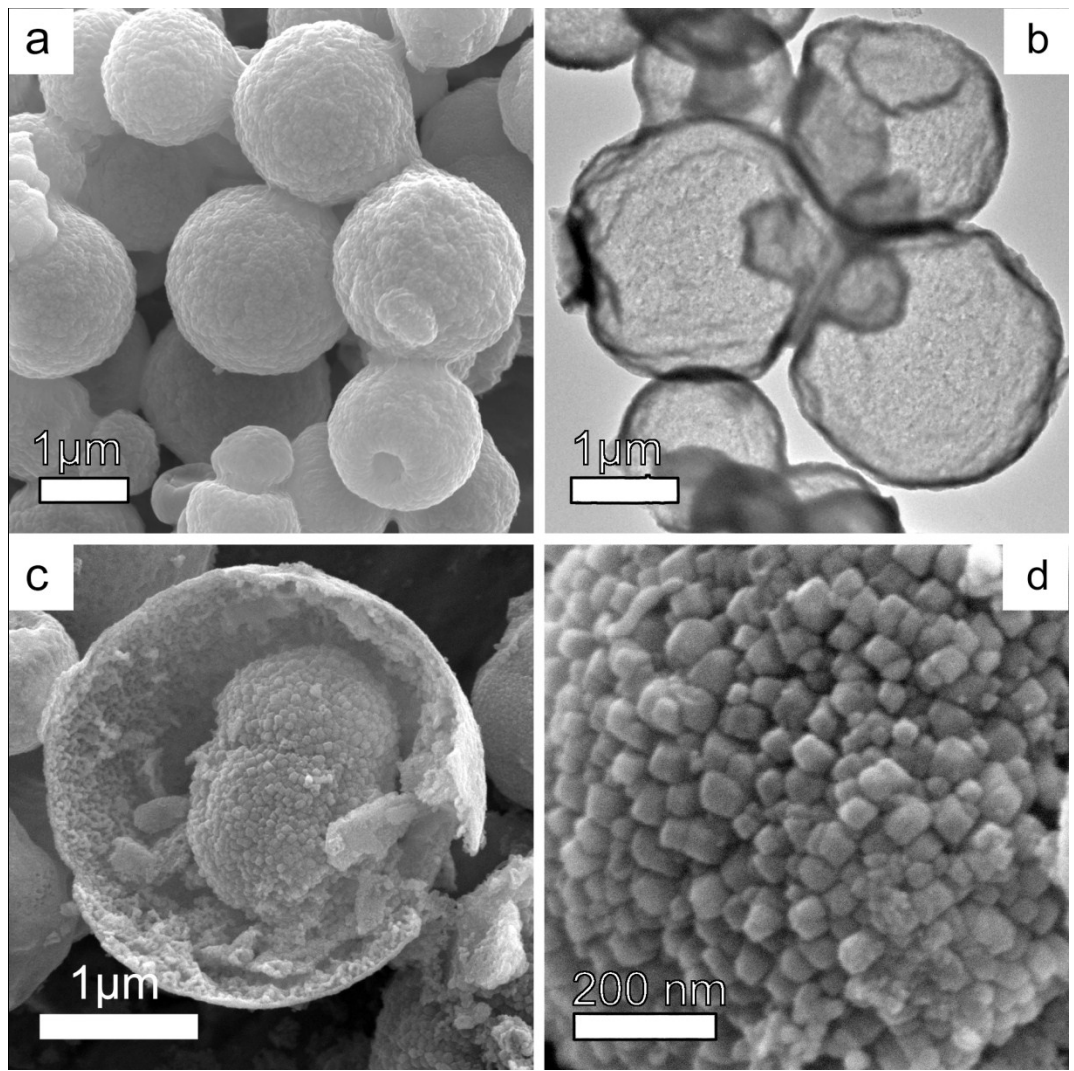


Fig. S5 (a) SEM image and (b) TEM image of as-synthesized HoMSS-T. (c) SEM image and (d) enlarged SEM image of as-synthesized HoMSS-S.

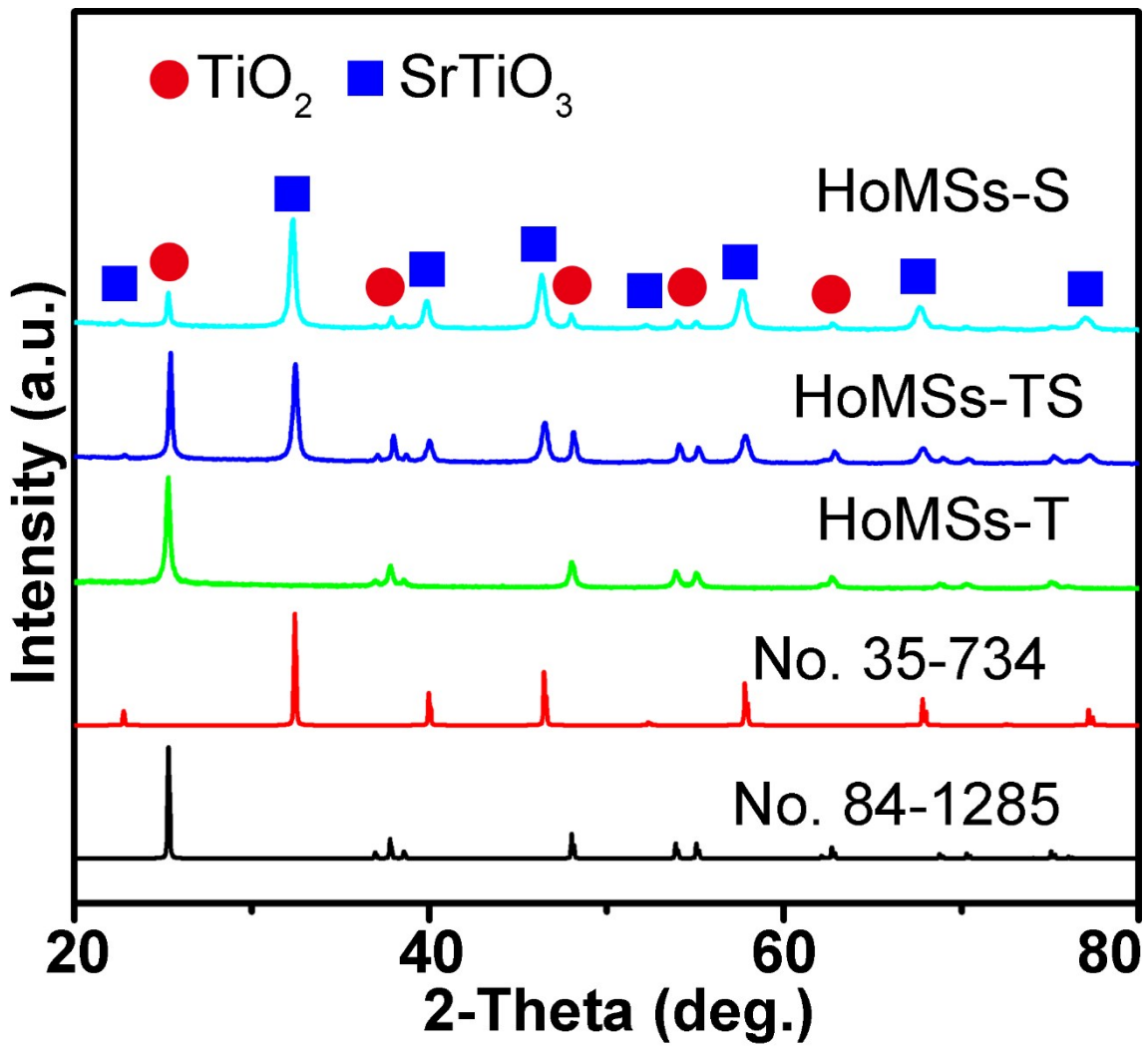


Fig. S6 XRD patterns of the different samples.

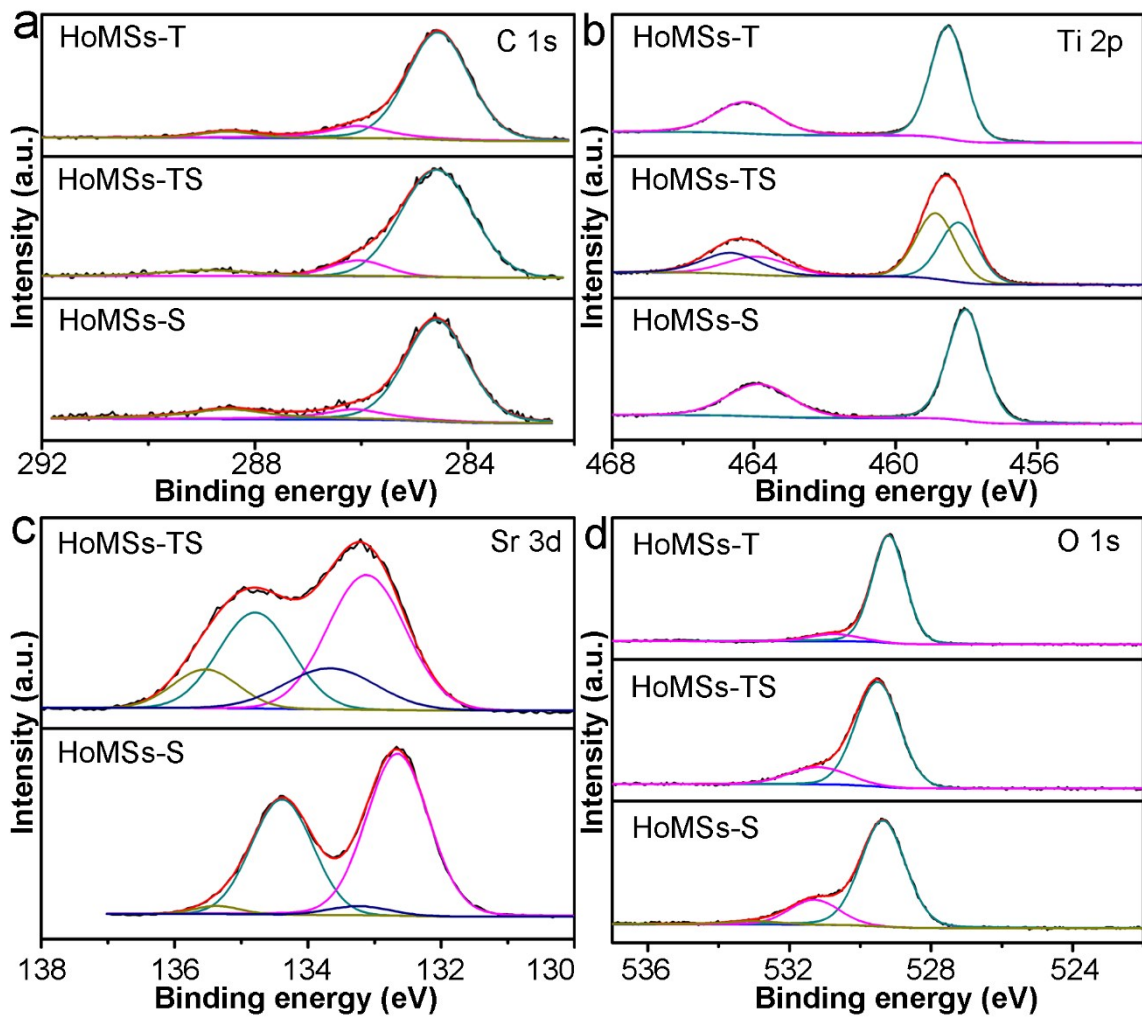


Fig. S7 XPS spectra of (a) C 1s, (b) Ti 2p, (c) Sr 3d, and (d) O 1s for the different samples.

Table S1 Summary of BET surface areas and BJH pore volumes of different samples

Sample name	BET surface areas ($\text{m}^2 \text{ g}^{-1}$)	BJH pore volumes ($\text{cm}^3 \text{ g}^{-1}$)
HoMSS-T	33	0.11
HoMSS-TS	42	0.15
HoMSS-S	23	0.09

Table S2 Summary of photocatalytic CO₂ reduction performances of different TiO₂- and SrTiO₃-based composites.

Photocatalyst	Reaction mode	Reactant	Major/minor products	Selectivity for CO ₂ reduction (%)	Reference
TiO ₂ /SrTiO ₃ spheres	Solid-gas	CO ₂ & H ₂ O vapor	CO/CH ₄	~100	Our work
Cr-SrTiO ₃	Solid-liquid	CO ₂ & H ₂ O	CH ₄	100	1
Rh-Au@SrTiO ₃	Solid-gas	CO ₂ & H ₂ O vapor	CO/H ₂	86	2
Pt-SrTiO _{3-δ}	Solid-gas	CO ₂ & H ₂ O vapor	CH ₄	100	3
SrTiO ₃ /ZnTe	Solid-gas	CO ₂ & H ₂ O vapor	CH ₄ /H ₂	-	4
TiO ₂ /SrTiO ₃ film	Solid-liquid	CO ₂ & 0.1 M KHCO ₃	CH ₄ /CO	-	5
Pt/SrTiO ₃ :Rh	Solid-liquid	CO/CO ₂ & 2 mM FeCl ₂	CH ₃ OH/H ₂	96	6
Cu _x O-SrTiO ₃	Solid-liquid	CO ₂ & 0.5M KHCO ₃	CO/H ₂	-	7
Au-SrTiO ₃	Solid-liquid	CO ₂ & H ₂ O vapor	CO/CH ₄	-	8
Pt-SrTi _{0.98} Co _{0.02} O ₃	Solid-gas	CO ₂ & H ₂ O vapor	CH ₄ /H ₂	90	9
Au ₃ Cu@SrTiO ₃ /TiO ₂	Solid-liquid	33.3% CO ₂ & hydrous hydrazine	CO/CH ₄ , C ₂ H ₆ , C ₂ H ₄ , C ₃ H ₆ , H ₂ , N ₂	-	10
TiO ₂	Solid-liquid	CO ₂ & H ₂ O	H ₂ /CO, CH ₄	19	
Pt-TiO ₂	Solid-liquid	CO ₂ & H ₂ O	H ₂ /CO, CH ₄	11	
TiO ₂	Solid-gas	CO ₂ & H ₂ O vapor	H ₂ /CO, CH ₄	56	
Pt-TiO ₂	Solid-gas	CO ₂ & H ₂ O vapor	H ₂ /CO, CH ₄	40	
Pd-TiO ₂	Solid-gas	CO ₂ & H ₂ O vapor	H ₂ /CO, CH ₄	42	11
Rh-TiO ₂	Solid-gas	CO ₂ & H ₂ O vapor	H ₂ /CO, CH ₄	45	
Au-TiO ₂	Solid-gas	CO ₂ & H ₂ O vapor	H ₂ /CO, CH ₄	41	
Ag-TiO ₂	Solid-gas	CO ₂ & H ₂ O vapor	H ₂ /CO, CH ₄	39	
MgO-Pt-TiO ₂	Solid-gas	CO ₂ & H ₂ O vapor	CH ₄ / H ₂ , CO	83	
TiO ₂	Solid-gas	CO ₂ & H ₂ O vapor	CH ₄ /H ₂	80	
Au/TiO ₂	Solid-gas	CO ₂ & H ₂ O vapor	CH ₄ /H ₂	94	12
Cu/TiO ₂	Solid-gas	CO ₂ & H ₂ O vapor	CH ₄ /H ₂	97	
(Au, Cu)/TiO ₂	Solid-gas	CO ₂ & H ₂ O vapor	CH ₄ /H ₂	97	

TiO ₂	Solid-liquid	CO ₂ & H ₂ O	H ₂	0
Au/TiO ₂	Solid-liquid	CO ₂ & H ₂ O	CH ₄ /H ₂	79
Cu/TiO ₂	Solid-liquid	CO ₂ & H ₂ O	CH ₄ /H ₂	91
(Au, Cu)/TiO ₂	Solid-liquid	CO ₂ & H ₂ O	CH ₄ /H ₂	92

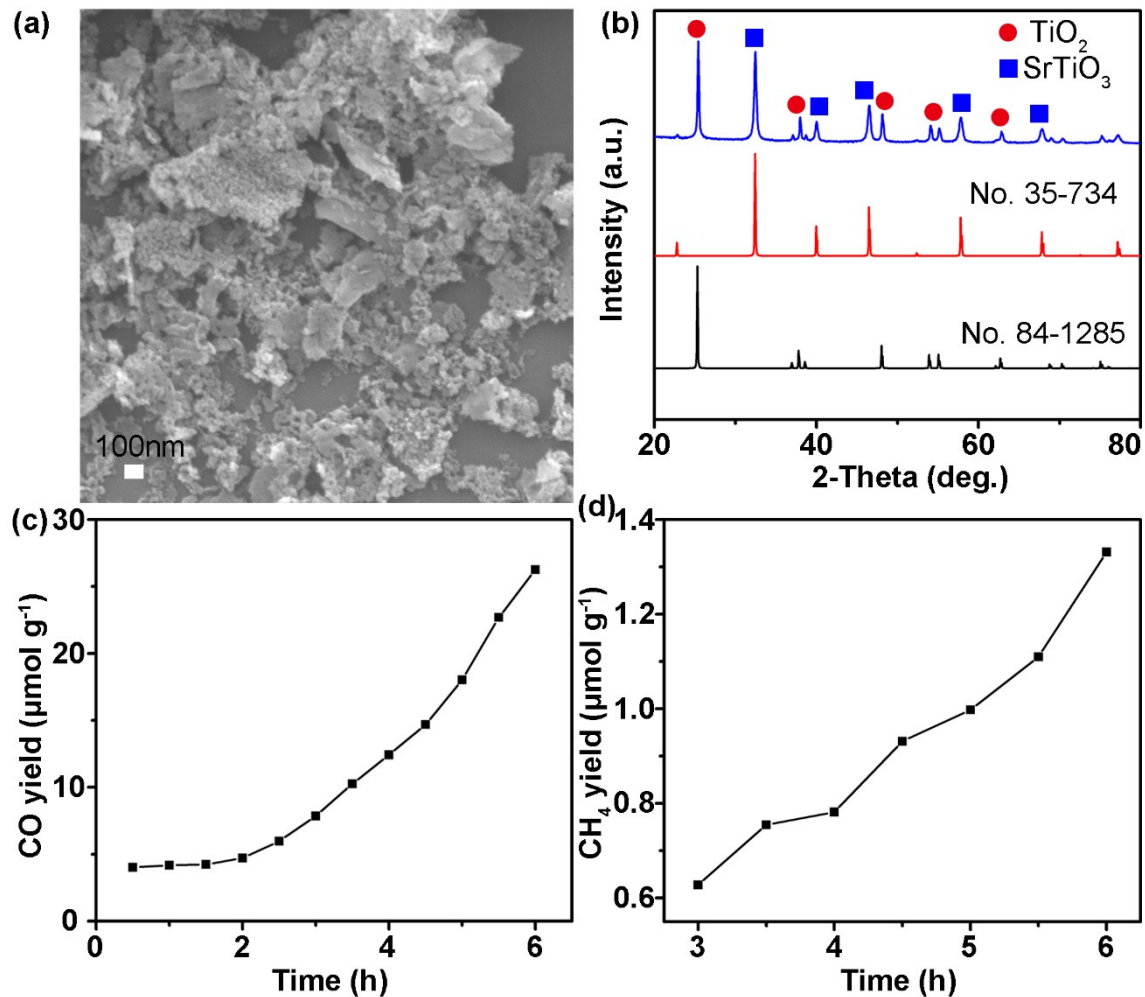


Fig. S8 (a) and (b) SEM image and XRD patterns of fragmentized $\text{TiO}_2/\text{SrTiO}_3$ sample(frg-TS), (c) and (d) CO and CH_4 yields of frg-TS under UV-vis irradiation. (Testing condition: 300 W Xe lamp, 320 nm $<\lambda < 780$ nm; catalyst: 5 mg coated on FTO with a geometric area of 4 cm^2 ; water 10 mL; mild reaction conditions (30°C and 1 atm CO_2)).

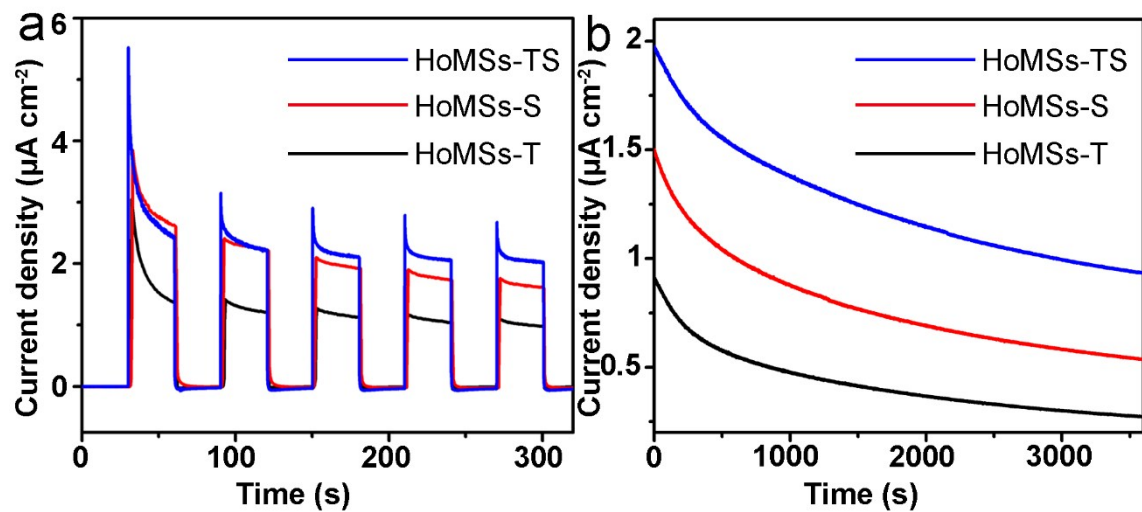


Fig. S9 (a) Transient photocurrent response curves measured under UV-vis irradiation using 0.1 M Na_2SO_4 as the electrolyte solution at a bias of 0.05 V vs. SCE for different samples, (b) Long-term photocurrent curves measured versus SCE as the reference electrode.

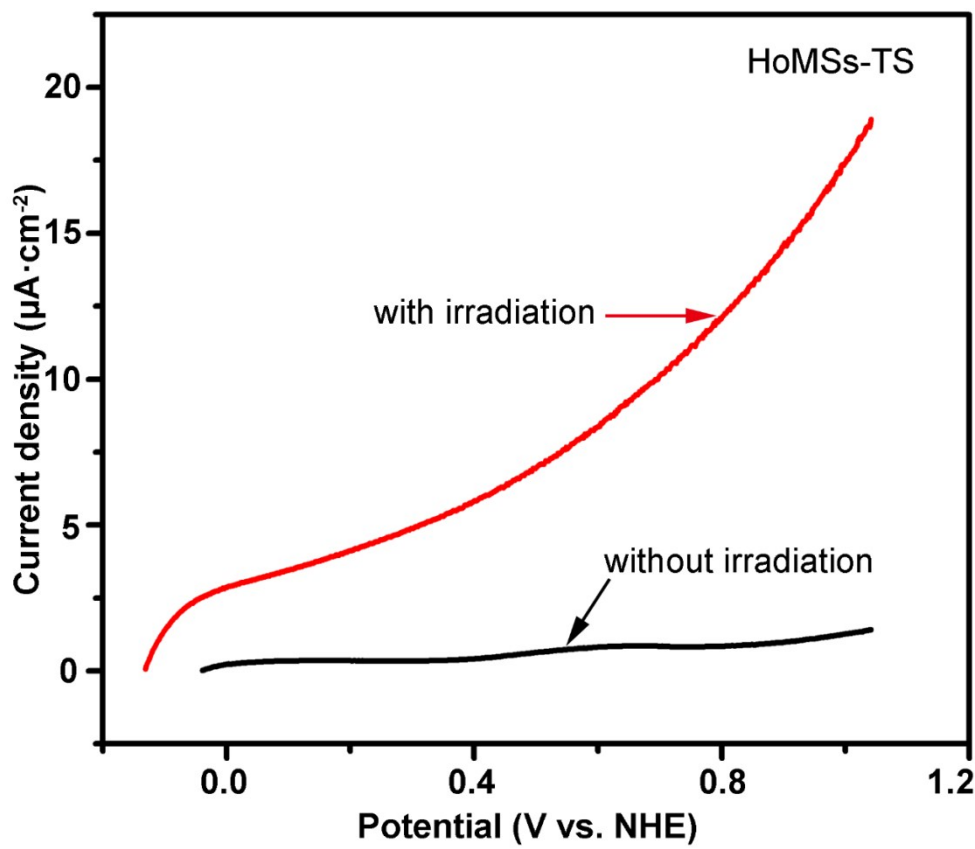


Fig. S10 Line scanning voltage (LSV) curves of HoMSs-TS measured with and without the irradiation of a 300 W Xe lamp, 0.1 M Na_2SO_4 as electrolyte solution, SCE and Pt as reference and counter electrode.

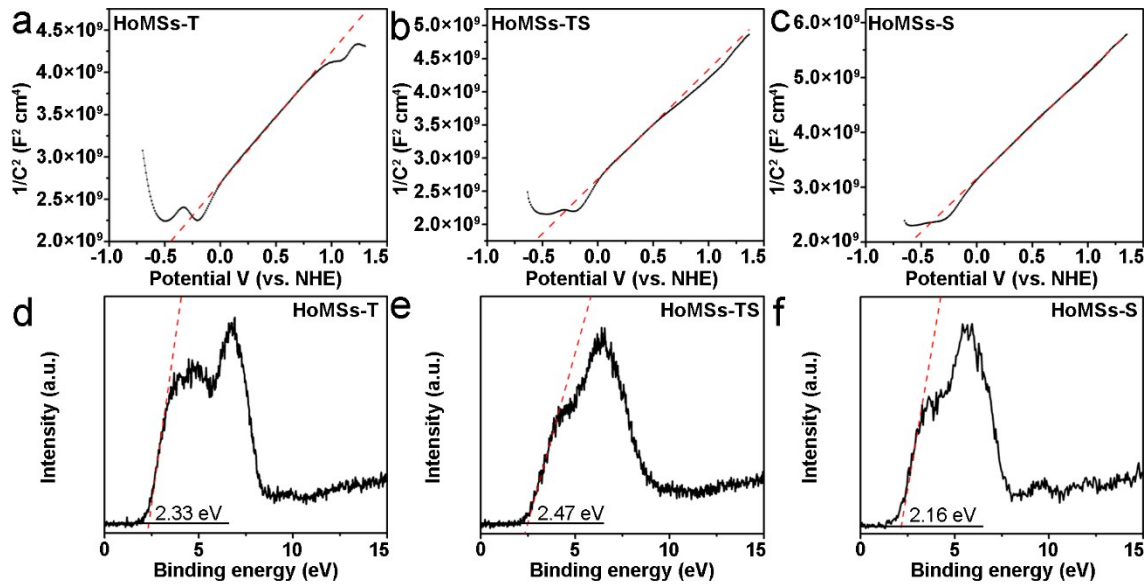


Fig. S11 Mott-Schottky plots and Valence band spectra of (a, d) HoMSS-T, (b, e) HoMSS-TS, and (c, f) HoMSS-S samples.

References

1. Y.Bi, M. F. Ehsan, Y. Huang, J. Jin, and T. He, *J. CO₂ Util.*, 2015, **12**, 43-48.
2. D. Li, S. Ouyang, H. Xu, D. Lu, M. Zhao, X. Zhang, and J. Ye, *Chem. Commun.*, 2016, **52**, 5989-5992.
3. K. Xie, N. Umezawa, N. Zhang, P. Reunchan, Y. Zhang, and J. Ye, *Energy Environ. Sci.*, 2011, **4**, 4211-4219.
4. M. F. Ehsan, M. N. Ashiq, F. Bi, Y. Bi, S. Palanisamy, and T. He, *RSC Adv.*, 2014, **4**, 48411-48418.
5. Y. Bi, L. Zong, C. Li, Q. Li, and J. Yang, *Nanoscale Res. Lett.*, 2015, **10**, 345.
6. Y. H. Cheng, V.H. Nguyen, H. Y. Chan, J. C. S. Wu, and W. H. Wang, *Appl. Energ.*, 2015, **147**, 318-324.
7. S. Shoji, G. Yin, M. Nishikawa, D. Atarashi, E. Sakai, and M. Miyauchi, *Chem. Phys. Lett.*, 2016, **658**, 309-314.
8. H. Zhou, J. Guo, P. Li, T. Fan, D. Zhang, and J. Ye, *Scientific Reports*, 2013, **3**, 1667.
9. J. Kou, J. Gao, Z. Li, H. Yu, Y. Zhou, and Z. Zou, *Catal. Lett.*, 2015, **145**, 640–646.
10. Q. Kang, T. Wang, P. Li, L. Liu, K. Chang, M. Li, and J. Ye, *Angew. Chem. Int. Ed.*, 2015, **54**, 841-845.
11. S. Xie, Y. Wang, Q. Zhang, W. Deng, and Y. Wang, *ACS Catal.*, 2014, **4**, 3644-3653.
12. S. Neațu, J. A. Maciá-Agulló, P. Concepción, and H. Garcia, *J. Am. Chem. Soc.*, 2014, **136**, 15969-15976.